Vol. 27: 301–311, 2002 | AQUATIC MICROBIAL ECOLOGY
Aquat Microb Ecol | Published April 16

A laboratory study on O_2 dynamics and photosynthesis in ice algal communities: quantification by microsensors, O_2 exchange rates, ^{14}C incubations and a PAM fluorometer

Ronnie N. Glud[1,*], Søren Rysgaard[2], Michael Kühl[1]

[1]Marine Biological Laboratory, Copenhagen University, Strandpromenaden 5, 3000 Helsingør, Denmark
[2]National Environmental Research Institute, Vejlsøvej 25, 8600 Silkeborg, Denmark

ABSTRACT: The present study compared O_2 exchange measurements, fluorometry and ^{14}C incubations for measuring productivity of sea-ice algae. It is demonstrated that brine leaking out of ice during freezing conditions is supersaturated with respect to O_2, while the melting water released during thawing is undersaturated with O_2. This results in a highly variable O_2 concentration at the ice-water interface during expanding or shrinking of sea ice. Consequently, great care should be taken when inferring biological activity from O_2 exchange rates, whether they are obtained via microprofiles, bulk incubations or direct measurement of O_2 concentrations in water below sea ice. Accounting for the O_2 dynamics related to changes in sea-ice structure, the photosynthetic activity of a mixed ice algal culture, as measured by net O_2 exchange rates and ^{14}C incubation, co-varied as a function of biomass and irradiance. The ratio between the net O_2 efflux and the gross C fixation rate (the photosynthetic quotient) was similar for frozen and non-frozen ice algal communities and averaged 1.43 ± 0.48. Quantification of the relative electron transport rate (ETR) from photosystem II (PSII) and the minimum fluorescence yield (F_0) by a pulse-amplitude-modulated (PAM) fluorometer offers a fast, simple and non-invasive approach for estimating activity and biomass of ice algal communities. The relative ETR measurements correlated with the other 2 measures for primary production. However, the correlation was non-linear, leading to a poor resolution of the fluorometer approach at higher photosynthetic activities. A similar observation was made for the correlation between measurements and the concentration of chlorophyll *a*.

KEY WORDS: Sea-ice algae · Primary production · Microelectrodes · Oxygen · Pulse amplitude modulated fluorometry · Fluorometer

INTRODUCTION

Sea-ice algae are an important component of marine polar ecosystems. Numerous studies have demonstrated that algal biomass accumulates within the ice matrix during spring and that the relative contribution of ice-related primary production can be significant (e.g. Horner & Schrader 1982, Palmisano & Sullivan 1983, Legendre et al. 1992, Grosselin et al. 1997, McMinn et al. 1999). Receding sea ice is also known to induce pelagic phytoplankton blooms due to freshwater-induced stratification of the water column, nutrient release and seeding of the water column (Smith & Nelson 1985, Nelson et al. 1987, Garrison & Buck 1989). In sub-polar regions or in coastal areas influenced by freshwater run off, the yearly contribution of ice algae to primary production may be less (Haecky & Andersson 1999, Rysgaard et al. 2001). However, their contribution during the spring bloom can still be

*E-mail: rnglud@zi.ku.dk

important, and here evidence for seeding is presented (Michel et al. 1993, Haecky et al. 1998).

Most measurements of primary production in sea ice have been obtained with modified versions of the ^{14}C incubation technique (Steenman-Nielsen 1952). This approach has the inherent problem that samples must be homogenized in order to determine the specific activity of the dissolved inorganic carbon (DIC). This is typically done by crushing the ice and adding filtered seawater or by thawing the sample prior to adding tracer. Both procedures change the microenvironmental controls on the photosynthetic activity: e.g. gradients of O_2, DIC and nutrient concentrations, salinity, temperature, microbial organization and light conditions. Samples are usually incubated in glass bottles placed under the ice in order to mimic the *in situ* light conditions. Recent measurements have, however, proved that this can be problematic due to enhanced irradiance in the vicinity of an ice edge or ice holes (Hansen et al. 2000). Incubation of ice slices placed in holes, sandwiched between the originally recovered ice blocks, may partly overcome this problem (Mock & Gradinger 1999). Nevertheless, the microscale optical properties of sea ice are complex, and scattering contributions to the light field experienced by the microalgae are very difficult to account for during incubations.

The ^{14}C incubation technique can at best be regarded only as a crude estimate of ice algal primary production. The photosynthetic activity within the complex and highly dynamic ice matrix may be very different from the rates extrapolated from bulk incubations, which are performed after changing the chemical and physical conditions of the community.

The shortcoming of the ^{14}C incubation technique for quantifying the primary production of ice algae has motivated the application of techniques well known from benthic research. Net O_2 exchange between ice and water has been used (e.g. Kuznetsov 1980), and recently O_2 exchange rates calculated from microelectrode profiles (McMinn & Ashworth 1998, McMinn et al. 2000) and pulse-amplitude-modulated (PAM) fluorometer measurements (Kühl et al. 2001, Rysgaard et al. 2001) were used for quantifying photosynthetic activity in intact ice algal communities. These techniques create minimum disturbance of the microenvironmetal conditions and are suitable for *in situ* application (see references above). Here we present a detailed comparison between the ^{14}C incubation technique and the recently introduced approaches in order to evaluate their potential and limitations in future studies on ice algae.

The aim of the present study was: (1) to evaluate the potential of O_2 exchange methods, microprofile measurements and PAM fluorometry for quantifying the photosynthetic activity of ice algal communities; (2) to intercalibrate these approaches with the ^{14}C incubation technique; and (3) to investigate the O_2 dynamics at the ice-water interface.

MATERIALS AND METHODS

Sampling, culturing and experimental set-up. Intact ice cores with ice algae were collected in September 1999 in the Fram Strait (74° 48.8′ N, 13° 44.1′ W). The ice cores were thawed in 0.22 µm filtered 32‰ seawater, and samples were transferred to culture vessels containing Drebes medium (von Storch & Drebes 1964) for enrichment of sea-ice microalgae. The obtained mixed algal culture was grown for approximately 2 mo at 2°C in 8 h dark:16 h light cycles. A halogen lamp kept the irradiance in the culture vessel at 20 µmol photons m^{-2} s^{-1}. The algae primarily developed on the sides of the culture vessel, and prior to dilution (every third week) the community was resuspended. Two weeks prior to the presented experiments the temperature was lowered to 0°C. The culture was dominated by diatoms (>95%) typical of ice algal communities: *Navicula* sp., *Nitzschia* sp., *Pinnularia* sp., *Gomphonema* sp. and *Stephanudiscus* sp. No significant changes in the taxonomic composition were observed during the experiments.

In order to ensure well-defined and reproducible samples for the intercalibration, the algal culture was suspended, and various volumes (0, 15, 25, 50, 75, 100, 150, 200 and 300 ml) were gently filtered onto a series of 22 mm GF/F filters. Filters were placed at the bottom of a series of cylindrical incubation vials (inner diameter [i.d.] 25 mm, height 30 mm) and approximately 18 ml of 0.22 µm filtered seawater was added. All measurements for the intercalibration of the 4 techniques were performed in these glass vials. For the first series, all vials were placed at the same irradiance provided by two 20 W halogen lamps (Phillips, BAN 9J) placed 1 m from the incubation vials. In another set-up with a parallel culture, 9 incubation vials with the same biomass (200 ml of suspended culture) were exposed to irradiances between 0 and 200 µmol photons m^{-2} s^{-1}. The desired irradiance was obtained by placing neutral density filters between the light source and the incubation vials.

All intercalibration measurements were performed in a thermostatically controlled laboratory. The first intercalibration experiment was performed without any ice present at 0°C. In the second intercalibration experiment only 3 ml of 0.22 µm filtered seawater was added, and the vials were placed on an aluminum bench cooled to –8°C. Overnight, the filters containing the algae froze into a 5 mm thick ice slice. Next day,

0.22 µm filtered seawater was added to fill the incubation vials. The algal community was thereby maintained in a stable temperature gradient (From 0 to −8°C). Small pieces of stainless steel placed in the vials kept the ice-encrusted algae from floating. As for the measurements performed without freezing, 2 series of vials were established in which the biomass and the irradiance, respectively, were varied. One complete experiment included a total of 36 incubation vials, containing either pure or ice-encrusted algal communities. All measurements were performed after a pre-incubation period of 2 to 4 h.

The biomass of the frozen algae increased over days to weeks under the experimental conditions. It was, however, difficult to maintain stable experimental conditions for several days or weeks. The growth of the ice-encrusted algae was very irregular, and this introduced a high degree of patchiness both between parallel samples and within a given sample. The physical appearance of the ice was very sensitive to even slight changes in temperature (or stirring), and it was impossible to maintain a constant ice volume during the incubations. Attempts to inoculate ice floes in larger containers, either directly or by freezing of algae-enriched GF/F filters from below, were only partly successful (see Fig. 1). Irregular patches of algae developed, and the biomass per area was relatively low. It was not possible to obtain large homogeneous algal communities suitable for an intercalibration study. However, the set-up was ideal for evaluating the O_2 dynamics below the ice. The temperature of the water bath and the ambient air could be regulated independently (±0.2°C), and consequently either freezing or thawing could be induced while microelectrode measurements were performed at the ice-water interface.

Fluorescence measurements. The relative photosynthetic electron transport rate (ETR), between photosystem II (PSII) and photosystem I (PSI), and the minimum fluorescence yield (F_0) were determined by a PAM fluorometer (Diving-PAM, Walz). The instrument quantifies chlorophyll fluorescence parameters by the 'saturation pulse method' (Schreiber et al. 1986, Bolhar-Nordenkampf et al. 1989). This approach is based on sample illumination with weak modulated probing pulses for monitoring the chlorophyll fluorescence yield without inducing actinic effects of the measuring light (Schreiber et al. 1986). Consequently, fluorescence can be measured independently of the actinic light, which can be orders of magnitude higher than the modulated probing light (Schreiber et al. 1986). The probing light, the actinic measuring light and the fluorescent signal were guided between instrument and sample by a 1 m long 8 mm fiber cable.

Fig. 1. Experimental set-up used to study the O_2 dynamics at the ice-water interface. The temperature of the water and air could be controlled independently (±0.2°C). Lower panel represents a close up of the upper panel

In dark-adapted algae, F_0 is measured as the community is exposed to the modulated measuring light. This weak fluorescence, emitted by the photosynthetic pigments, can be used as a proxy for algal biomass (Serodio et al. 1997, Rysgaard et al. 2001). Exposing the sample to actinic light, provided by an internal halogen lamp in the instrument, results in an elevated fluorescence yield (F). Subsequent exposure of the light-adapted sample to a very intense saturation pulse leads to a maximum PSII fluorescence yield (F_m). With-

out any additional pulsing, the fluorescence gradually reversed to the original *F*-value. The relative ETR between PSII and PSI for a given sample can be calculated as follows:

$$\mathrm{ETR} = \frac{(F_m - F)}{F_m} E_0(\mathrm{PAR})$$

where E_0(PAR) is the scalar irradiance of photosynthetically active radiation. This simple approach assumes that the absorption cross-section of PSII (σ_a) is constant during the measurements (Hofstraat et al. 1994). Exposing an algal community to changing light conditions can lead to a gradual adaptation of the photosynthetic apparatus by changes in σ_a (Kolber & Falkowski 1993). However, construction of rapid light curves (RLC), where the community is exposed to each actinic light level for only 10 to 20 s, provides a snapshot of the current status of the photosynthetic apparatus at the ambient light conditions without interference from a transient adaptation (Schreiber et al. 1997, Ralph et al. 1999). Only RLC measurements are presented in this study, and all measurements used for the intercalibration were performed with the 8 mm fiber head touching the algal communities or the ice-water interface. PAM fluorometry measurements can be truly non-invasive by placing a spacer ring around the fiber head, preventing the fiber from touching the sample, but this approach was not applied in the present study. A detailed presentation and discussion of the fluorometer approach for investigating ice algae is given elsewhere (Kühl et al. 2001, Rysgaard et al. 2001).

Measurements of O_2 microprofiles and total O_2 exchange rates. In order to quantify the diffusive O_2 exchange (DOE) between algae and ambient water, O_2 microprofiles were measured with Clark-type microelectrodes (Revsbech 1989). Due to the risk of breaking sensors against ice crystals, the outer glass casing was reinforced and the outside diameter of the applied sensors was in the order of 50 to 200 µm. The internal sensor hole was, however, only a few micrometers, ensuring good measuring characteristics of the electrodes, i.e. stirring sensitivities <1% and a 90% response time <2 s (Revsbech 1989, Glud et al. 2000). There was no significant difference in the data obtained by sensors of various thickness. The vertical position of the sensors was controlled at a 100 µm depth resolution using a motor-driven micromanipulator. The sensor current was measured with a picoammeter connected to an analog to digital (A/D) converter that transferred the signals to a PC (Revsbech & Jørgensen 1986). During measurements the water phase was stirred by a small internal magnet fixed to the wall of the incubation vials. The magnet received momentum from a rotating external magnet, controlled via a small 12 V direct current (DC) motor. Continuous air flushing of the water phase ensured 100% air saturation during the measurements.

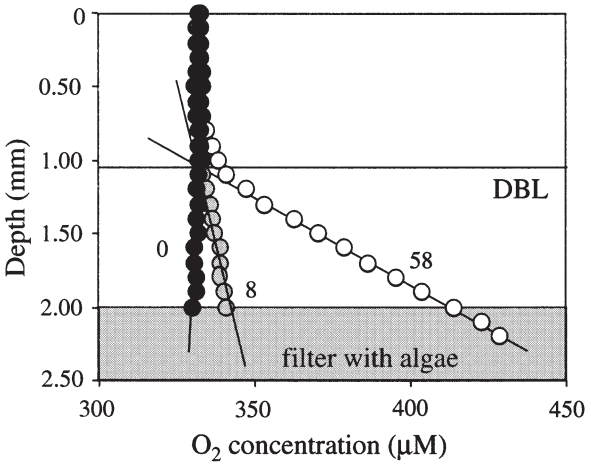

Fig. 2. Three O_2 microprofiles measured in the water above an ice algal community fixed on a GF/F filter under 3 different irradiances (3, 8 and 58 µmol photons m^{-2} s^{-1}). The linear gradients measured within the diffusive boundary layer (DBL) were used to calculate the diffusive O_2 exchange (DOE) of the community

O_2 concentration profiles measured through the apparent diffusive boundary layer (Fig. 2) were used to calculate the DOE by applying Fick's first law of diffusion: $\mathrm{DOE} = -D_0\,\delta C/\delta Z$, where D_0 is the molecular diffusion coefficient and C is the O_2 concentration at depth Z (Fig. 2) (Crank 1983). The diffusion coefficient was derived from Broecker & Peng (1974) and corrected for temperature as described by Li & Gregory (1974). The approach assumes that diffusion is the only transport mode across the interface. This is not always the case in ice-encrusted communities, were especially salinity-dependent density gradients can induce advection and percolation (e.g. Hsiao 1988).

After microprofiling, the total O_2 exchange (TOE) between algal communities and water was quantified. Incubations were initiated by sealing the vials with transparent Plexiglas lids. The vials were subsequently placed at the respective irradiances and stirring of the water phase was maintained as described above. After incubations the O_2 concentration was determined by removing the lids and inserting a calibrated O_2 microelectrode in the overlying water. During the approximately 3 h long incubations, the O_2 concentrations changed by 2 to 25% depending on biomass and experimental conditions. The TOE between algae and water was calculated from measured concentration changes accounting for the volume of the enclosed water phase.

^{14}C incubations and chlorophyll *a* determinations. Prior to sealing the incubation chambers for determination of the TOE, 4 µCi $H^{14}CO_3^-$ was added to each of the incubation vials. After incubation (see above), subsamples for the determination of the DIC concentration were transferred to gas-tight exetainers spiked with saturated $HgCl_2$ and later analyzed on a Coulometer (CM5012). Subsequently, the content of the vials (water and ice) was filtered onto a 22 mm GF/F filter. The filtered sample and the original filter were divided into 2 equal-sized fractions for determination of the chlorophyll *a* (chl *a*) concentration and the amount of fixed $H^{14}CO_3^-$, respectively. For primary production measurements the samples were transferred to scintillation vials, and inorganic carbon was removed by addition of 200 µl 1 N HCl and subsequent air flushing of the vials. Scintillation fluid was added and samples were counted after 24 h. Primary production rates were calculated after correcting for the fixation rates in dark-incubated samples (Steenman-Nielsen 1952). The other half of the sample was extracted with 96% ethanol (Jespersen & Christoffersen 1987) and the chl *a* concentration was measured spectrophotometrically (Strickland & Parsons 1972).

RESULTS

For the algal communities incubated at 0°C, the O_2 exchange derived from the total incubations and calculated from the measured microprofiles gave very similar results (Fig. 3A,B). The O_2 release rate increased almost linearly with the chl *a* content of the filters when exposed to an irradiance of 30 µmol photons m^{-2} s^{-1} (Fig. 3A). When communities with a chl *a* content of 162 ± 31 mg m^{-2} were exposed to increasing irradiance, the O_2 release rate showed light saturation around 75 µmol photons m^{-2} s^{-1}, but no inhibition was observed (Fig. 3B). Primary production rates derived from the ^{14}C fixation technique performed in the same incubation vials as the O_2 exchange measurements were similar (Fig. 3A,C & 3B,D). The ratio between the net O_2 release and the gross DIC fixation rate in the various vials (the apparent photosynthetic quotient [PQ]) was mostly above 1 with an average value of 1.44 ± 0.47 (n = 15) (Fig. 4A).

The relative ETR exhibited a faster saturation with increasing biomass compared to the other 2 approaches (Fig. 3E,F). The RLC of the communities adapted to 30 µmol photons m^{-2} s^{-1} showed a steep increase with the irradiance, and light saturation was observed at irradiances around 40 µmol photons m^{-2} s^{-1}. A non-linear relation between the relative ETR measurements and the other 3 measures for primary production is apparent in Fig. 4B. The F_0 value as a

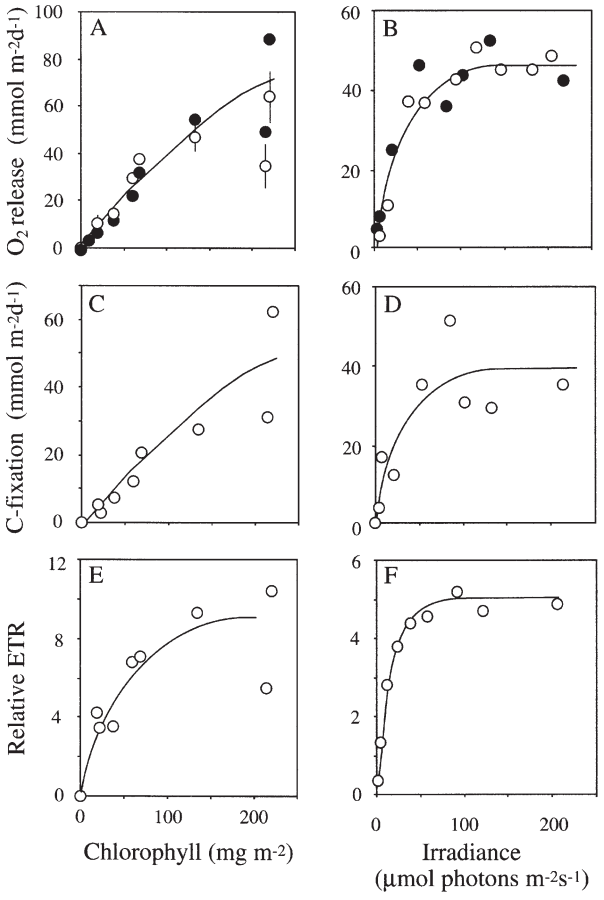

Fig. 3. (A,B) Total (●) and diffusive (○) O_2 exchange rate as a function of the chlorophyll *a* (chl *a*) content and the irradiance of ice algal communities fixed on GF/F filters. (C,D) Inorganic carbon fixation rate and (E,F) relative electron transport rate (ETR) of the same communities. The irradiances in (F) are the actinic light imposed by the internal halogen lamp of the fluorometer. The irradiance in (A), (C) and (E) was 30 µmol photons m^{-2} s^{-1} and the chl *a* content in (B), (D) and (F) was 162 ± 31 mg m^{-2}. Vertical bars through symbols indicate the standard deviation and are included in (A) and (B) (n = 3); in most cases they are smaller than the symbol size. All lines were hand drawn

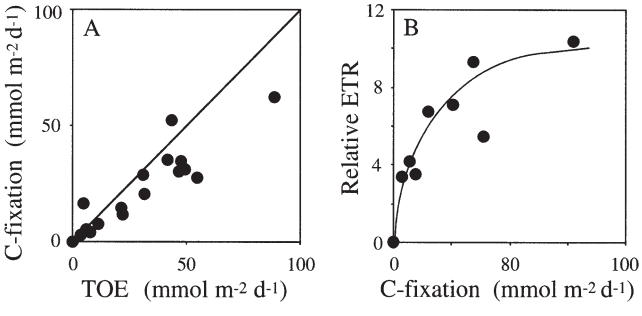

Fig. 4. (A) Inorganic carbon fixation rate as a function of the total O_2 exchange rate presented in Fig. 3A,B. The line $x = y$ is included. (B) Relative ETR as a function of the carbon fixation rate presented in Fig. 3C,E; the curve was hand drawn

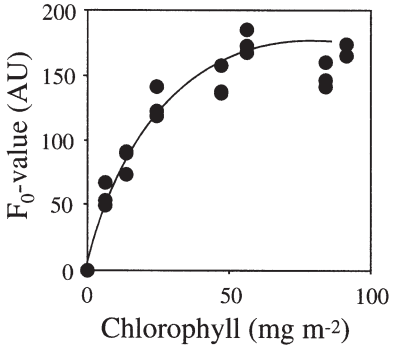

Fig. 5. Minimum fluorescence yield (F_0), as a function of the chl *a* concentration of the ice algal community. The curve was hand drawn

function of the chl *a* content also showed saturation, leading to a poor signal resolution at high biomass (Fig. 5).

Measurements of O_2 microprofiles in the ice-encrusted algae demonstrated a high spatial variability of O_2 concentration at the ice-water interface (Fig. 6A). Neighboring profiles measured within a distance of a few millimeters could indicate either significant export, no exchange or import of O_2 (Fig. 6A). Consequently, the standard deviation on the average DOE for a given sample was high, and meaningful production estimates would require an unrealistically high number of O_2 microprofiles to be measured. With 10 repetitive measurements there was no apparent correlation between the DOE and biomass or irradiance (data not shown). Microprofiles obtained in pure ice without any biological activity also reflected a high spatial and temporal variability in the O_2 concentration. In a set-up where temperature could be accurately controlled (Fig. 1), microelectrode measurements performed below developing ice demonstrated an elevated signal close to the ice-water interface, indicating O_2 release (Fig. 6B). In thawing ice we made the opposite observation: the signal decreased as the sensor approached the ice-water interface (Fig. 6B).

The TOE measured in the incubation vials integrated the spatial heterogeneity resolved with the microsensors, and the rate increased almost linearly with increasing biomass (Fig. 7A). However, negative rates in pure ice and in vials with low biomass reflected an O_2 decrease during the incubations. Despite many attempts to maintain steady ice conditions within the vials during incubations, it was impossible to maintain a constant ice volume. For the presented data it was observed that at the end of the incubations some ice had thawed. For ice-encrusted samples with a biomass of 159 ± 46 mg chl *a* m^{-2} the TOE generally increased with increasing irradiance, but also here thawing of samples was associated with a negative O_2 exchange

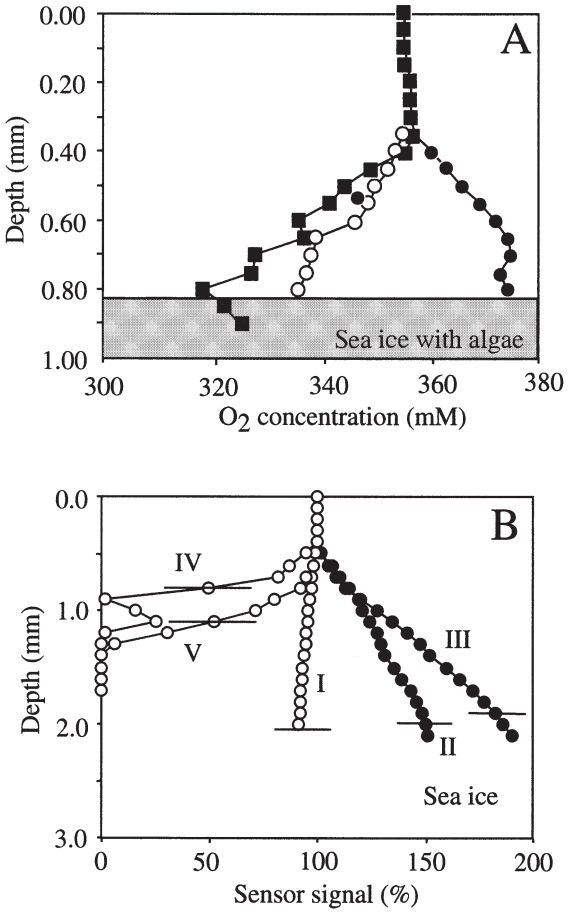

Fig. 6. (A) O_2 microprofiles measured within 1 cm^2 of an ice-encrusted algal community under identical environmental conditions but with changing ice structure during the measurements. Different symbols mark repetitive measurements. (B) O_2 microprofiles measured in pure ice. Profiles were measured as the ice grew (I, II, III) or during thawing (IV, V). Horizontal lines indicate the position of the ice-water interface for the respective profiles

rate (Fig. 7B). The ^{14}C incubations performed in the same vials as the TOE measurements revealed a gradual increase in primary production with increasing biomass (Fig. 7C) and similar observations were made for samples exposed to increasing irradiance (Fig. 7D). Data obtained in ice-encrusted samples were generally more scattered than data from incubations performed at 0°C. However, plotting the primary production rates calculated from the ^{14}C incubations against the TOE still indicated a linear correlation (Fig. 8). By ascribing the TOE measured in vials containing only pure ice (–8.9 mmol m^{-2} d^{-1}) to the O_2 deficiency arising from thawing during incubations, the photosynthetic activity in the ice-encrusted algae could be quantified. Adding the non-biological O_2 deficit to the ice algae-containing vials incubated in parallel re-

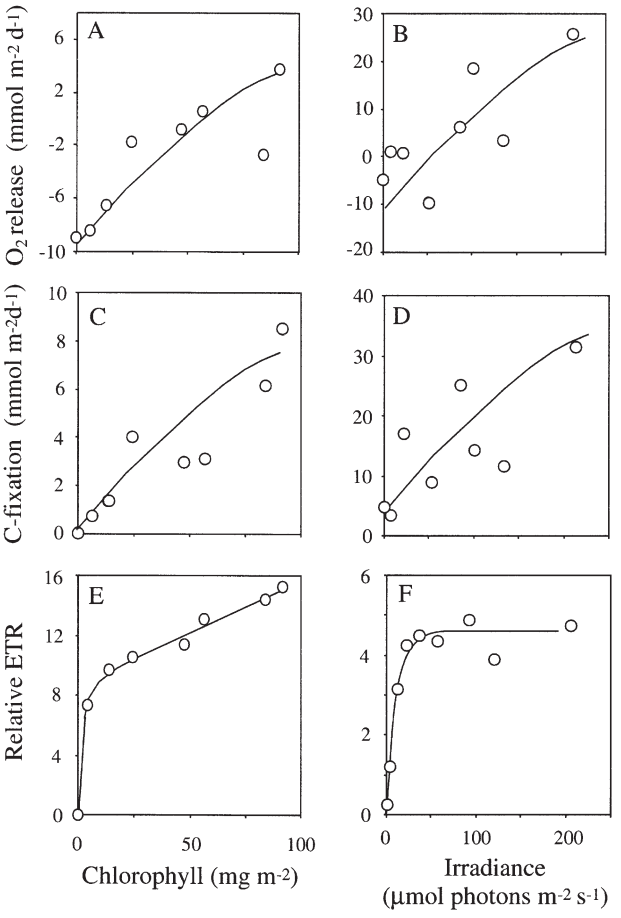

Fig. 7. (A,B) Total O_2 exchange rate as a function of chl *a* content and irradiance of ice-encrusted ice algal communities fixed on GF/F filters. (C,D) Inorganic carbon fixation rate and (E,F) relative ETR of the same communities. The irradiances in (F) are the actinic light imposed by the internal halogen lamp of the fluorometer. The irradiance in (A), (C) and (E) was 46 µmol photons m^{-2} s^{-1} and the chl *a* content in (B), (D) and (F) was 159 ± 46 mg m^{-2}. (n = 3). Lines were hand drawn

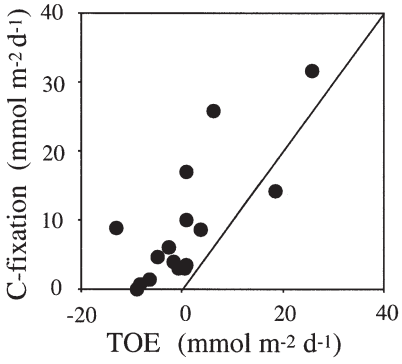

Fig. 8. Inorganic carbon fixation rate as a function of the total O_2 exchange rate presented in Fig. 7A,B. The line $x = y$ is included

sulted in a PQ of 1.42 ± 0.49 (n = 16). This was similar to the ratio obtained for the incubations performed at 0°C.

As for the measurements performed at 0°C, the relative ETR increased with the chl *a* content, up to 100 mg m^{-2}. Also, the response of the relative ETR toward increasing irradiance was similar in samples kept below and above the freezing point of seawater (Figs. 3F & 7F). Generally, the relative ETR indicated a lower scatter than the other measures of primary production (Figs. 3 & 7).

Measurements with the PAM fluorometry fiber cable positioned at variable distances above an ice algal sample fixed on a GF/F filter showed that fluorescence signals could be detected several millimeters away (Fig. 9A). It was observed that the signal approximately doubled when the distance was reduced by 2 mm (Fig. 9A). Measurements before and after freezing of an overlying water film of 5 mm revealed a decrease in signal equivalent to the increase in distance between fiber and algal community (Fig. 9B,C).

DISCUSSION

O_2 dynamics in sea ice

The presented data clearly demonstrated that O_2 microelectrodes changed signal as they approached an ice matrix without biological activity. However, apart from the O_2 concentration, several physical and chemical parameters can affect the signal of O_2 microelectrodes (Glud et al. 2000). The applied sensors had a stirring sensitivity of <1% and, consequently, effects of changing flow velocity on the sensor signals could be ignored. However, since microelectrodes measure the partial pressure of O_2, changes in temperature and salinity affect the sensor signal even if the O_2 concentration is constant (Gundersen et al. 1998, Glud et al. 2000). In a separate set-up, the O_2 concentration was kept constant, and signal changes induced by changes in salinity and temperature were quantified. The sensor signal increased almost linearly by 5% per 1°C and 0.2% per 1‰ salinity increase in the relevant range (0 to 10°C and 0 to 60‰, respectively; data not shown). A recently presented mathematical model that predicts the signal change of Clark-type O_2 microelectrodes due to changes in salinity and temperature confirmed these results (Gundersen et al. 1998, Glud et al. 2000). In developing or thawing sea ice, the 2 effects partly counteract each other since the temperature and salinity gradients have opposite signs. The effects undoubtedly affected our O_2 microelectrode measure-

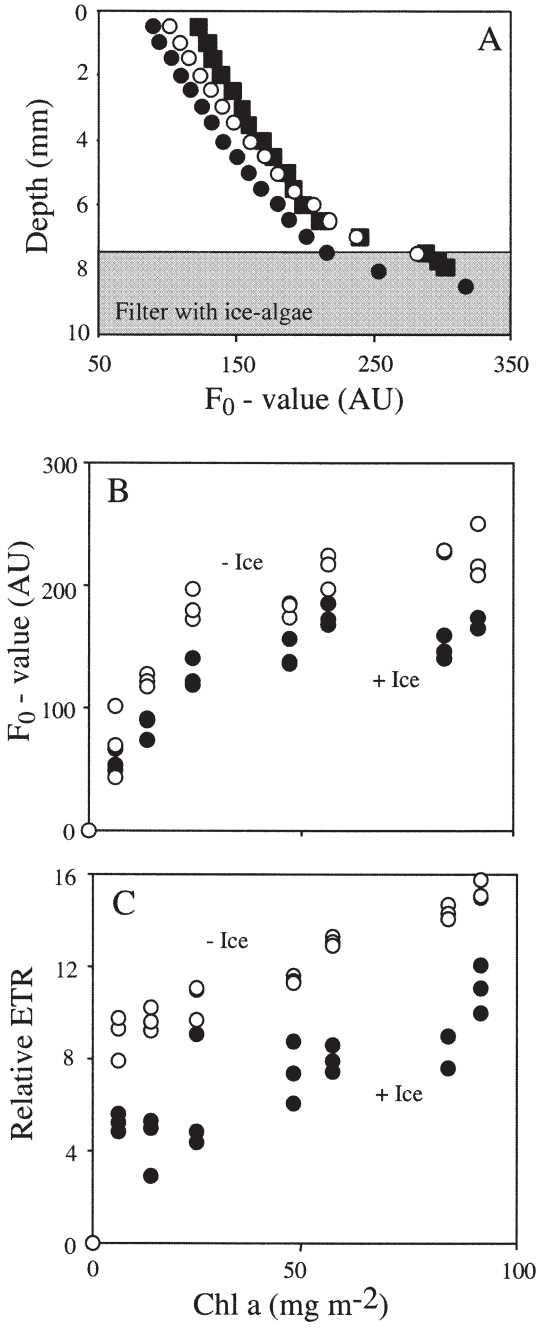

Fig. 9. (A) F_0 value measured in water at variable distance between sample and fiber-optics. Different symbols represent repetitive measurements. (B,C) F_0 value and relative ETR measured at the surface of the same ice algal community with and without ice cover as a function of the chl *a* of the filters. Three repetitive measurements were performed on each sample

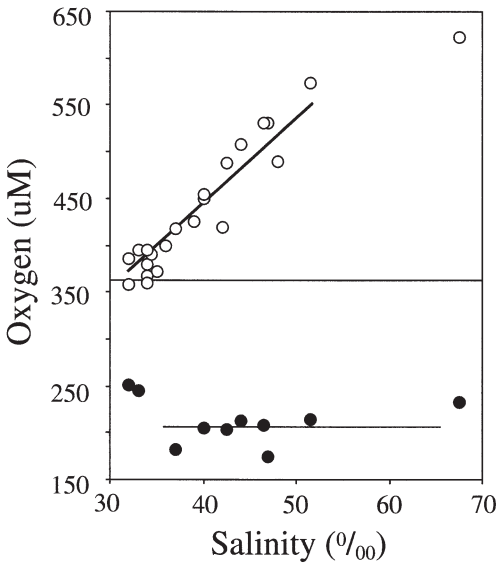

Fig. 10. Total O_2 concentration in water below a growing ice flake (○) and in the ice matrix (●) as a function of the salinity in the underlying water. The horizontal line indicates the O_2 concentration of the isolated water prior to any freezing. Lines were hand drawn

ments but cannot alone explain the very steep gradients observed in this study (e.g. Fig. 6B).

In another experiment, the salinity and O_2 concentration (as determined by Winkler titration) in the water below developing sea ice was measured over time (see Fig. 1). As expected, the salinity increased in the underlying water volume as concentrated brine leaked out of the growing ice. However, the O_2 concentration increased in parallel (Fig. 10). Thawing of the ice matrix showed that melting water from the sea ice had low O_2 concentrations (Fig. 10). These data confirmed the observation made with microelectrodes that brine leaking out of sea ice is supersaturated, while melting water is undersaturated with respect to O_2. Essentially, O_2 and presumably other gasses (CO_2 and N_2) behave in the same way as ionic solutes. The major part of O_2 associated with the sea-ice matrix was most likely trapped in gas bubbles that developed during the freezing process. Quantifying the volume of the entrapped gas bubbles and performing a simple mass balance calculation indicated that the gas bubbles on average also were undersaturated with respect to O_2. There is, however, no simple way to determine the absolute O_2 concentration within the entrapped bubbles. We speculate that the O_2 depletion associated with ice thawing creates favorable conditions for anaerobic bacteria and processes (e.g. denitrification, sulfate reduction) within the ice matrix.

In coastal settings the physical appearance of the ice-water interface can be highly dynamic depending on changes in air temperature, wind speed, solar radiation and precipitation (Rysgaard et al. 2001). Direct *in situ* measurements with O_2 microelectrodes performed in Young Sound, NE Greenland, showed an extreme spatial and short-term temporal variability in O_2 concentra-

tion at the ice-water interface (Kühl et al. 2001, Rysgaard et al. 2001). Under such circumstances great care should be taken when inferring biological activity from O_2 exchange measures, whether they are obtained by microprofiling, bulk incubations or direct measurement of the O_2 concentration in water under the sea ice. At steady state, O_2 dynamics related to changes in ice structure may be less, and good correlations between irradiance and *in situ* O_2 evolution quantified by microsensors have been presented from environments at quasi-steady state (McMinn et al. 2000).

Microprofile measurements toward solid ice revealed a very sharp decrease in the signal, which presumably was caused by physical blocking of the diffusive O_2 supply to the sensor. It was also observed that as the sensor tip touched the ice, changes in the local hydrodynamics (Glud et al. 1994) induced local erosion of the ice crystal, and the sensor gradually melted its way through the ice. Another aspect that needs attention for more precise quantification of exchange rates below sea ice is the very poorly defined transport coefficients within the ice matrix and at the ice-water interface. This is, however, beyond the scope of the present study.

There was a reasonable linear correlation between O_2 exchange measurements and ^{14}C incubations both in ice-encrusted and in non-frozen communities. When negative TOE values were corrected for the O_2 depletion related to ice thawing, the combined data set revealed a PQ of 1.43 ± 0.48. This is not significantly different from the generally accepted value of 1.2 (Strickland & Parsons 1972), which may vary depending on the nutritional status of the community (e.g. Williams et al. 1979). A ratio below 1.2 was actually expected as the ^{14}C approach quantifies gross primary production, while the O_2 exchange rate represents the net primary production of the community. This may indicate that for the given culture a significant fraction of the electrons derived from the splitting of water were used for purposes other than CO_2 reduction. For practical purposes it was not possible to perform the intercalibration in cultures well established within an ice matrix, and it remains to be seen whether the good agreement between the O_2 exchange method (corrected for the contribution from changes in ice structure) and ^{14}C incubations also holds for natural ice algal communities.

Fluorescent parameters as measures for biomass and primary production in sea ice

The fluorescence parameters obtained with the PAM fluorometer are volumetric measures of the activity and the biomass of microalgae, respectively. However, the absolute size of the integrated volume is poorly defined. Since the surface-associated culture is exposed to the pulsed probing light from above, the light is primarily absorbed in the upper layer of the community. For optical reasons, the fluorescence emitted by the surficial community also has a higher probability of being captured and recorded by the instrument than does the fluorescence from algae positioned in the deeper layers (Walz 1998). This self-shading effect changes the volume over which the signal is integrated as the biomass is increased and results in a saturating, non-linear relation between F_0 and chl *a* concentration. Similarly, the relative ETR represents mainly the response of the surficial community. In a surface-associated community, the very upper algae may be light inhibited while the community as such still can increase its photosynthetic activity (Kühl et al. 1997). This is probably the reason for the very steep increase of the *PE* (Photosynthesis vs Irradiance) curves measured by the PAM fluorometer as compared to *PE* curves obtained by other activity measures that integrate the signal of the complete community (light saturated and non-saturated algae). It is therefore to be expected that in less dense ice algal communities, the relation between the relative ETR and the TOE or the ^{14}C incubation becomes more linear.

Another geometric effect of the PAM fluorometry approach is that the intensity of the areal excitation light decreases with the distance from the fiber head. This, together with the decreasing probability of catching the fluorescent signal, leads to a distance-dependent signal (Fig. 9). *In situ* ice often has steep gradients in chl *a* concentration (e.g. Cota & Smith 1991) and to what extent various algae contribute to the measured fluorescence is very dependent on their position and the optical properties of the sea ice. In our set-up the PAM fluorometer could measure the fluorescence from algae positioned in a well-defined layer 1 to 2 cm inside clear sea ice.

Measuring the relative ETR and F_0 is a simple and fast method for non-invasive quantification of the temporal and spatial variability of fluorescent parameters of intact communities of sea-ice algae (Rysgaard et al. 2001). It is, however, important to realize that these parameters are only proxies for primary production and biomass, respectively. The PSII ETR is closely coupled to the O_2 production and a good correlation between these parameters has been found for both microalgae and macroalgae (Henley 1993, Hanelt et al. 1995, Hartig et al. 1998). However, under non-optimal conditions, highly variable and non-linear relations have been reported (Flameling & Kromkamp 1998). The knowledge about the relationship between PSII electron transport and O_2 production is limited and further work on the effects of microenvironmental controls on this relation is required (e.g. Schreiber et al. 2002). A close relationship between PSII electron transport and CO_2 fixation cannot be expected as elec-

trons can be used for cyclic electron transport or other metabolic processes, rather than CO_2 reduction. Nevertheless, a good linear correlation between ^{14}C incubations and ETR has been reported for benthic microphytes (Barranguet & Kromkamp 2000).

In order to transform the fluorescence parameters into more applicable measures such as O_2 production, C fixation and chl *a* density, it is necessary to obtain empirical relations between PAM measurements and the more traditional approaches for measuring primary production in ice algae. Since we have little insight into how the various parameters co-vary, it is necessary to construct such correlations often and within the environment during a field campaign. As a consequence, fluorometer-based primary production estimates become no better than the techniques to which they are calibrated.

In the present study the relative ETR was determined assuming a constant absorption cross-section of PSII (σ_a). Since samples were preincubated at constant irradiance for hours prior to any measurements, this requirement was fulfilled in the presented data (see e.g. Ralph et al. 1999). Measuring the relative ETR at variable time intervals (0.5 to 3 min) after changing the actinic irradiance showed that the investigated community had the ability to adapt quickly to changes in irradiance (data not shown). Similar observations were made for intact ice algal communities *in situ* (Kühl et al. 2001, Rysgaard et al. 2001). RCLs give a snapshot of the current status of light adaptation of the community; while the ^{14}C incubation and the O_2 exchange approach integrate a signal over several hours. For intercalibration performed in the field at changing irradiance this has to be considered. For diel or seasonal studies where changes in σ_a are to be expected, frequent intercalibration between PAM measurements and the other approaches is required.

Another approach for quantifying the ETR of PSII in aquatic systems is the so-called 'pump and probe method' (Falkowski et al. 1986). By this approach it is possible to estimate σ_a directly (Kolber & Falkowski 1993), and after the recent development of an *in situ* fast repetition rate fluorometer (Gorbunov et al. 2000), the technique is an alternative procedure for quantifying fluorescent parameters of intact ice algal communities.

Conclusion

We showed that sea-ice microbial communities experience highly variable O_2 concentration during freezing or thawing of the ice-brine matrix. O_2 dynamics associated with physical changes of sea ice have to be accounted for when using O_2 exchange rates as a measure for biological activity in sea ice. Gross photosynthesis inferred from ^{14}C incubations and net photosynthesis determined by O_2 exchange rates co-varied as a function of irradiance and biomass of an ice algal community. The absolute rates did, however, suggest that a significant fraction of the electrons derived from the splitting of water was used for other purposes than CO_2 reduction. Alternative incubation techniques accounting for the non-biological-related O_2 dynamics in sea ice should be developed in order to obtain better *in situ* estimates of the primary production of sea-ice algal communities. The relative ETR and the F_0 value correlated well with the other measures for primary production and biomass, but self-shading within the algal community resulted in non-linear relations at high biomass. Depending on the density of the algal communities, the PAM measurements provided an integrated value for approximately the lower 1 to 2 cm of an ice core. Further work on the correlation between fluorescent parameters and photosynthetic activities in O_2 or C equivalents is required.

Acknowledgements. This study was financed by the Danish National Science Research Council and the Carlsberg Foundation. A. Glud is thanked for constructing the applied O_2 microelectrodes. We thank K. Meiners and R. Gradinger for providing the ice algal cultures applied in this study. Two anonymous reviewers are also thanked for constructive and helpful criticism.

LITERATURE CITED

Barranguet C, Kromkamp J (2000) Estimating primary production rates from photosynthetic electron transport in estuarine microphytobenthos. Mar Ecol Prog Ser 204:39–52

Bolhar-Nordenkampf HR, Long SR, Baker NR, Öquist G, Schreiber U, Lechner EG (1989) Chlorophyll fluorescence as a probe of the photosynthetic competence of leaves in the field; a review of current instrumentation. Funct Ecol 3:497–514

Broecker WS, Peng TH (1974) Gas exchange rates between air and sea. Tellus 26:21–35

Cota GF, Smith REH (1991) Ecology of bottom ice algae: II. Dynamics, distributions and productivity. J Mar Syst 2:279–295

Crank J (1983) The mathematics of diffusion. Clarendon Press, Oxford

Falkowski PG, Wyman K, Ley AC, Mauzerall DC (1986) Relationship of steady state photosynthesis to fluorescence in eucaryotic microalgae. Biochem Biophys Acta 849:183–192

Flameling IA, Kromkamp J (1998) Light dependence of quantum yields for PSII charge separation and oxygen evolution in eucaryotic algae. Limnol Oceanogr 43:284–297

Garrison DL, Buck KR (1989) The biota of Antarctic pack ice in the Weddell Sea and Antarctic Peninsular regions. Polar Biol 10:211–219

Glud RN, Gundersen JK, Revsbech NP, Jørgensen BB (1994) Effects on the benthic diffusive boundary layer imposed by microelectrodes. Limnol Oceanogr 39:462–467

Glud RN, Gundersen JK, Ramsing NB (2000) Electrochemical and optical oxygen microsensors for *in situ* measurements. In: Buffle J, Horvai G (eds) *In situ* analytical techniques for water and sediment. John Wiley and Sons, Chichester, p 19–75

Gorbunov MY, Falkowski P, Kolber Z (2000) Measurements of

photosynthetic parameters in benthic organisms *in situ* using a SCUBA-based fast repetition rate fluorometer. Limnol Oceanogr 45:242–245

Grosselin M, Levasseur M, Wheeler P, Horner R, Boot B (1997) New measurements of phytoplankton and ice algae production in the Arctic Ocean. Deep-Sea Res 44:1623–1644

Gundersen JK, Glud RN, Ramsing NB (1998) Predicting the signal of O_2 microsensors from physical dimensions, salinity and O_2 concentration Limnol Oceanogr 43:1932–1937

Haecky P, Andersson A (1999) Primary and bacterial production in sea ice in the northern Baltic sea. Aquat Microb Ecol 20:107–118

Haecky P, Jonsson S, Andersson A (1998) Influence of sea ice on the composition of the spring phytoplankton bloom in the Northern Baltic Sea. Polar Biol 20:1–8

Hanelt D, Uhrmacher S, Nultsch W (1995) The effect of photoinhibition on photosynthetic oxygen production in the brown algae *Dictyota dichotoma*. Bot Acta 108:99–105

Hansen JW, Rysgaard S, Laursen JS (2000) Primary production of ice algae and phytoplankton in a high Arctic fjord: light artifacts when measuring from a hole in the sea ice. American Society of Limnology and Oceanography 2000, Waco (Poster presentation)

Hartig P, Wolfstein K, Lippemeier S, Colijn F (1998) Photosynthetic activity of natural microphytobenthos populations measured by fluorescence (PAM) and ^{14}C-tracer methods: a comparison. Mar Ecol Prog Ser 166:153–164

Henley WJ (1993) Measurement and interpretation of photosynthetic light-response curves in algae in the context of photoinhibition and diel changes. J Phycol 29:729–739

Hofstraat JW, Peeters JCH, Snel JFH, Geel C (1994) Simple determination efficiency and photoinhibition of *Dunaliella tertiolecta* by saturation pulse fluorescence measurements. Mar Ecol Prog Ser 103:187–196

Horner R, Schrader GC (1982) Relative contribution of ice algae, phytoplankton, and benthic microalgae to primary production in nearshore regions of the Beaufort Sea. Arctic 35:485–503

Hsiao SIC (1988) Spatial and seasonal variations in primary production of sea ice microalgae and phytoplankton in Frobisher Bay, Arctic Canada. Mar Ecol Prog Ser 44:275–285

Jespersen AM, Christoffersen K (1987) Measurements of chlorophyll a from phytoplankton, using ethanol as extraction solvent. Arch Hydrobiol 109:445–454

Kolber Z, Falkowski PG (1993) Use of fluorescence to estimate phytoplankton photosynthesis *in situ*. Limnol Oceanogr 38:1646–1665

Kühl M, Lassen C, Revsbech NP (1997) A simple light meter for measurements of PAR (400 to 700 nm) with fiber-optic microprobes: application for P vs E_0 (PAR) measurements in a microbial mat. Aquat Microb Ecol 13:197–207

Kühl M, Glud RN, Borum J, Roberts R, Rysgaard S (2001) Photosynthetic performance of surface-associated algae below sea ice as measured with a pulse amplitude-modulated (PAM) fluorometer and O_2 microsensors. Mar Ecol Prog Ser 223:1–14

Kuznetsov LL (1980) Chlorophylls and primary production associated with ice of Amour Bay, Sea of Japan. Sov J Mar Biol 6:297–299

Legendre L, Ackley SF, Dieckmann GS, Gulliksen B and 6 others (1992) Ecology of sea ice biota. 2. Global significance. Polar Biol 12:429–444

Li YH, Gregory S (1974) Diffusion of ions in deep-sea sediments. Geochim Cosmochim Acta 38:703–714

McMinn A, Ashworth C (1998) The use of oxygen microelectrodes to determine the net production by an Antarctic sea ice algal community. Antarct Sci 10:39–44

McMinn A, Ashworth C, Ryan K (1999) Growth and productivity of Antarctic sea ice under PAR and UV irradiances. Bot Mar 42:401–407

McMinn A, Ashworth C, Ryan K (2000) *In situ* net primary productivity of an Antarctic fast ice bottom algae community. Aquat Microb Ecol 21:177–185

Michel C, Legendre L, Therriault JC, Demers S, Vandevelde T (1993) Springtime coupling between ice algae and phytoplankton assemblages in the southeastern Hudson Bay, Canadian Arctic. Polar Biol 13:441–449

Mock T, Gradinger R (1999) Determination of Arctic ice algae production with a new *in situ* incubation technique. Mar Ecol Prog Ser 177:15–26

Nelson DM, Smith WO, Gordon LI, Huber BA (1987) Spring distribution of density, nutrients and phytoplankton biomass in the ice edge zone of the Weddell-Scotia Sea. J Geophys Res 92:7181–7190

Palmisano AC, Sullivan CW (1983) Sea ice microbial communities (SIMCO). 1. Distribution, abundance and primary production of microalgae in McMurdo Sound, Antarctica in 1980. Polar Biol 2:171–177

Ralph PJ, Gademann R, Larkum AWD, Screiber U (1999) *In situ* underwater measurements of photosynthetic activity of coral zooxanthellae and other reefdwelling dinoflagellate endosymbionts. Mar Ecol Prog Ser 180:139–147

Revsbech NP (1989) An oxygen microelectrode with a guard cathode. Limnol Oceanogr 34:474–478

Revsbech NP, Jørgensen BB (1986) Microelectrodes and their use in microbial ecology. Adv Microb Ecol 9:293–352

Rysgaard S, Kühl M, Glud RN, Hansen JW (2001) Biomass, production and horizontal patchiness of sea ice algae in a high-Arctic fjord (Young Sound, NE Greenland). Mar Ecol Prog Ser 223:15–26

Schreiber U, Schliwa U, Bilger W (1986) Continuous recording of photochemical and non-photochemical chlorophyll fluorescence quenching with a new type of modulation fluorometer. Photosynth Res 10:51–62

Schreiber U, Gademann R, Ralph PJ, Larkum AWD (1997) Assessment of photosynthetic performance of *Prochloron* in *Lissoclinum patella in hospite* by chlorophyll fluorescence measurements. Plant Cell Physiol 38:945–951

Schreiber U, Gademann R, Bird P, Ralph PJ, Larkum AWD, Kühl M (2002) Apparent light requirement for activation of photosynthesis upon rehydration of desiccated beachrock microbial mats. J Phycol 38:125–134

Serodio J, da Silva JM, Cataina F (1997) Nondestructive tracing of migratory rhythms of intertidal benthic microalgae using *in vivo* chlorophyll a fluorescence. J Phycol 33: 542–553

Smith WE, Nelson DM (1985) Phytoplankton bloom produced by a receding ice edge in the Ross Sea: coherence with the density field. Science 227:163–166

Steenman-Nielsen E (1952) The use of radio-active carbon (^{14}C) for measuring organic production in the sea. J Cons Int Explor Mer 18:117–140

Strickland JDH, Parsons TR (1972) A practical handbook of sea water analysis. Bull Fish Res Board Can 167:1–310

von Storch HA, Drebes G (1964) Entwicklungsgeschichtliche Untersuchungen an zentrischen Diatomeen. IV. Die Planktondiatomee *Stephanopyxix turris*, ihre Behandlung und Entwicklungsgeschichte. Helgol Wiss Meeresunters 11: 209–257

Walz H (1998) Underwater fluorometer diving PAM—a handbook of operation. Heinz Walz, Effeltrich

Williams PJL, Raine RCT, Bryan JR (1979) Agreement between the ^{14}C and oxygen methods of measuring phytoplankton production: reassessment of the photosynthetic quotient. Oceanol Acta 2:411–416

Editorial responsibility: William Li, Dartmouth, Nova Scotia, Canada

Submitted: July 9, 2001; Accepted: January 30, 2002
Proofs received from author(s): March 27, 2002